Microscopic Analysis of the Elastic Properties of Nebulin in Skeletal Myofibrils

Kenji Yasuda,* Takashi Anazawa,‡ and Shin'ichi Ishiwata‡

*Advanced Research Laboratory, Hitachi Ltd., Hatoyama, Saitama 350-03, Japan, and ‡Department of Physics, School of Science and Engineering, Waseda University, 3-4-1 Okubo, Shinjuku-ku, Tokyo 169, Japan

ABSTRACT The elastic properties of nebulin were studied by measuring the elasticity of single skeletal myofibrils, from which the portion of the thin filament located at the I band had been selectively removed by treatment with plasma gelsolin under rigor conditions. In this myofibril model, a portion of each nebulin molecule at the I band was expected to be free of actin filaments and exposed. The length of the exposed portion of the nebulin molecule was controlled by performing the gelsolin treatment at various sarcomere lengths. The relation between the passive tension and extension of the exposed portion of the nebulin showed a convex curve starting from a slack length, apparently in a fashion similar to that of wool. The slack sarcomere length shifted depending on the length of the exposed portion of the nebulin, however, the relation being represented by a single master curve. The elastic modulus of nebulin was estimated to be two to three orders of magnitude smaller than that of an actin filament. Based on these results, we conclude that nebulin attaches to an actin filament in a side-by-side fashion and that it does not significantly contribute to the elastic modulus of thin filaments. The relation between the passive tension and extension of connectin (titin) was obtained for a myofibril from which thin filaments had been completely removed with gelsolin under contracting conditions; this showed a concave curve, consistent with the previous results obtained in single fibers.

INTRODUCTION

The contractile system of muscle requires an elastic framework to maintain its organized structure (for recent reviews, cf. Small et al., 1992; Ebashi, 1991). Recent studies have demonstrated that an exceptionally giant protein called connectin (titin) (Maruyama, 1986; Wang, 1985) is elastic so as to be responsible for the passive tension generation in stretched muscle fibers (Funatsu et al., 1990, 1993; Wang et al., 1993) and for positioning thick filaments at the center of each sarcomere (Horowits and Podolsky, 1987). As directly observed by electron microscopy after the selective removal of thin filaments from single skeletal muscle fibers (Funatsu et al., 1990) and a bundle of cardiac muscle (Funatsu et al., 1993), connectin (titin) filaments connect the ends of thick filaments and the Z line. Also, connectin (titin) has attracted attention because it is a candidate for the length-regulating ruler of thick filaments (Wang and Wright, 1988; Whiting et al., 1989; Trinick, 1992).

On the other hand, another giant protein called nebulin was recently found and suggested to be located along a thin filament (Wang and Wright, 1988). It has also attracted attention because it is a plausible candidate for the regulator of thin filament length (Kruger et al., 1991; Jin and Wang, 1991; Labeit et al., 1991; Wright et al., 1993; Pfuhl et al., 1994). In relation to its physiological function, it is interesting that nebulin is absent from cardiac muscle (Wang and Wright, 1988; Itoh et al., 1988); this seems to reflect the fact that the length of thin filaments is not strictly regulated (Robinson and Winegrad, 1977). It is important to examine the elastic properties of nebulin, because nebulin is considered to be a scaffold, as well as a template protein, that is responsible for stabilization and length determination of the filaments (Wang and Wright, 1988; Trinick, 1992; Wright et al., 1993; Pfuhl et al., 1994). From a physiological point of view, the extent to which nebulin contributes to the elastic modulus of thin filaments is also an important issue.

Viscoelastic properties of the elastic elements such as connectin (titin) in muscle fibers have been extensively studied using single fibers, skinned mechanically (Natori, 1954) or chemically (cf. Magid and Law, 1985). Recently, we have succeeded in manipulating single myofibrils under an optical microscope and measuring the tension development on the order of nanonewtons (Anazawa et al., 1992). The present study was designed to examine the structure and function of nebulin, using the above system.

To study the mechanical properties of these giant myofibrillar proteins, we used plasma gelsolin (brevin), an actin-binding protein possessing the ability to sever an actin filament, as a molecular tool for selectively removing thin filaments (cf. Funatsu et al., 1990, 1993). New types of contractile systems have been obtained with gelsolin treatment under rigor conditions and subsequently under contracting conditions; the models thus obtained appeared to be suitable for studying the mechanical properties of nebulin and connectin (titin) separately. A preliminary report of this work was presented previously (Yasuda et al., 1992).

Received for publication 11 May 1994 and in final form 29 July 1994.

Address reprint requests to Dr. Shin'ichi Ishiwata, Department of Physics, School of Science and Engineering, Waseda University, 3-4-1 Okubo, Shinjuku-ku, Tokyo 169, Japan. Tel.: 81-3-3203-4141; Fax: 81-3-3200-2567; E-mail: ishiwata@cfi.waseda.ac.jp.

Abbreviations used: BDM, 2,3-butanedione 2-monoxime; DFP, diisopropyl fluorophosphate; MOPS, 3-(*N*-morpholino) propanesulfonic acid.

Mr. Anazawa's current address: Central Research Laboratory, Hitachi Ltd., Kokubunji, Tokyo 185, Japan.

0006-3495/95/02/598/11 $2.00

MATERIALS AND METHODS

Solutions

Solution A: 60 mM KCl, 5 mM $MgCl_2$, 10 mM Tris-maleate (pH 6.8), and 1 mM EGTA; rigor (−Ca) solution: 0.15 M KCl, 1 mM $MgCl_2$, 10 mM 3-(*N*-morpholino)propanesulfonic acid (MOPS) (pH 7.0), 1 mM EGTA, 2 mM diisopropyl fluorophosphate (DFP), and 2 mM leupeptin; rigor (+Ca) solution: the above rigor (−Ca) solution containing 0.1 mM $CaCl_2$ instead of 1 mM EGTA; relaxing solution, 0.12 M KCl, 4 mM $MgCl_2$, 4 mM ATP, 20 mM MOPS (pH 7.0), 2 mM EGTA, 2 mM DFP, and 2 mM leupeptin with or without 20 mM 2,3-butanedione 2-monoxime (BDM); rigor-gelsolin (RG-) solution, 0.15 M KCl, 1 mM $MgCl_2$, 10 mM MOPS (pH 7.0), 0.1 mM $CaCl_2$, 2 mM DFP, 2 mM leupeptin, and 0.1 mg/ml gelsolin; contraction-gelsolin (CG-) solution: 0.15 M KCl, 5 mM $MgCl_2$, 4 mM ATP, 10 mM MOPS (pH 7.0), 0.1 mM $CaCl_2$, 2 mM DFP, 2 mM leupeptin, and 0.1 mg/ml gelsolin. ATP was purchased from Boehringer Mannheim GmbH (Mannheim, Germany), MOPS from Dojindo (Kumamoto, Japan), DFP and BDM from Wako Pure Chemical Industries Ltd. (Osaka, Japan), leupeptin from Peptide Institute Inc. (Osaka, Japan). Other chemicals were of reagent grade.

Preparation of myofibrils

Single or a small bundle of skeletal myofibril was prepared by homogenizing rabbit psoas glycerinated muscle fibers as described previously (1 mM leupeptin was added to the glycerol solution); the homogenization was done in solution A using a homogenizer (IKA-WERK T-18 type, 8G, Staufen, Germany) (Ishiwata and Funatsu, 1985; for further detail, see Ishiwata et al., 1993). The diameter of the single or the small bundle of skeletal myofibril used in the present work ranged from 1.5 to 3.7 μm. The number of sarcomeres between a pair of glass micro-needles (cf. Figs. 1, 3, and 9) was 25–40. Cardiac myofibrils (used in Fig. 2 only) were prepared from bovine papillary glycerinated muscle using a similar procedure (for further detail, see N. Fukuda, T. Fujita, and S. Ishiwata, unpublished data). Myofibrils thus prepared were stored in solution A at 0°C and used on the same day.

Preparation of plasma gelsolin

Plasma gelsolin (brevin), a calcium-dependent, actin-binding, and actin-severing protein (Yin and Stossel, 1979; Harris and Weeds, 1984), was purified from bovine plasma using a rapid, simple procedure developed by Kurokawa et al. (1990); bovine plasma was fractionated with 35–50% $(NH_4)_2SO_4$ in the presence of 50 mM Tris-HCl (pH 8. 0) and 0.1 mM DFP (E-64 was omitted), and then dialyzed against a Ca^{2+}-free solution. Plasma gelsolin was bound to a DE-52 (Whatman Biosystems Inc., Maidstone Kent, U.K.) column in the Ca^{2+}-free solution and eluted by increasing the concentration of Ca^{2+}. The purification procedure was repeated once more, using the same column. Plasma gelsolin thus obtained showed a single band corresponding to a molecular weight of about 90 kDa on SDS-PAGE.

Microscopic system for tension measurement and structure analysis

The microscopic system used for measuring tension development and for analyzing the internal structure of myofibrils was essentially the same as described previously (Anazawa et al., 1992), except that a piezo element was used for stretching a myofibril by controlling displacement of a stiffer glass micro-needle. In brief, the system consists of the following parts: (1) temperature-controlled cell (about 200 μl) in which a myofibril is fixed to a pair of glass micro-needles, one of which is flexible (Hooke's elastic constant, 0.22–1.06 μg/μm) and the other is rigid (~300 μg/μm); (2) micromanipulators with a piezoelectric element (PSt 150/50/5, Dr. Lutz Pickelmann, Munich, Germany); (3) an inverted phase-contrast microscope (DIAPHOT-TMD; Plan Apo 60 X oil DM objective lens [1.40 NA] for measuring tension and for taking the micrographs and density profiles shown in Figs. 1, 3, and 9; Nikon Co., Ltd., Tokyo) equipped with a CCD-camera (C3077H, Hamamatsu Photonics K. K., Hamamatsu, Japan); and (4) a video-computer system for image analysis. The developed tension and the average sarcomere length were estimated by measuring the deflection of the flexible needle and the separation between the inner edges of the two micro-needles by using a double-channel position detector (Width analyzer C3161, Hamamatsu Photonics K. K.). The developed tension of myofibrils and the fine structure of sarcomeres were determined simultaneously and recorded on a video tape recorder; a density profile of the recorded image of a myofibril was analyzed afterward by an image processor (Slot vision, Mitani Shouji K. K., Tokyo). The entire system was controlled by a personal computer (PC9801, NEC Co., Ltd., Tokyo). Space and time resolutions (spatial resolution, 50 nm; time resolution, 1/30 s) were limited mainly by the recording system. The binding of fluorescence dye-labeled actin to myofibrils was examined under an optical microscope (Fluophoto VFD-R; CF Plan 100 X oil DM objective lens [1.25 NA] for Fig. 2; Nikon Co., Ltd.). Tri-X films (Eastman Kodak Co., Rochester, NY) were used for taking phase-contrast and fluorescence micrographs (Microdol-X developer diluted 1:3; Eastman Kodak Co.).

Preparation of several models of myofibrils

We prepared the following two types of artificial models of myofibrils. First, a myofibril in which the portion of the thin filament located at the I band was selectively removed with gelsolin treatment for 10 min in an RG-solution (we call this model an *RG-treated* myofibril). Second, a myofibril from which thin filaments, other than the short fragments located at the Z line, were selectively removed by a two-step gelsolin treatment in an RG-solution and then in a CG-solution for 5 min (we call this model a *CG-treated* myofibril). This two-step procedure is essentially the same as that used in the previous study on muscle fibers (Funatsu et al., 1990). These models of myofibrils, both ends of which had been held by a pair of glass micro-needles, were observed under phase-contrast and fluorescence microscopes (Fig. 1).

The selective removal of thin filaments was confirmed by staining with 0.33 μM rhodamine phalloidin (Molecular Probes Inc., Eugene, OR) after chemical fixation in each solution containing 3% formaldehyde for 30 min (cf. Figs. 1 and 2; Funatsu et al., 1990). To identify the thin filaments without damaging mechanical and contractile properties of myofibrils, staining with 0.33 μM rhodamine phalloidin was done in each solution without chemical fixation (cf. Fig. 3). In this case, only the free (pointed) ends of thin filaments and the Z line were labeled (cf. Funatsu et al., 1990). In case of skeletal myofibrils, the staining was done after holding the myofibrils with a pair of glass micro-needles. All procedures were done in the cell at room temperature (about 25°C).

Preparation of labeled actin

Actin was prepared from acetone powder that had been prepared from rabbit leg and back white muscle according to a standard procedure (cf. Ishiwata and Funatsu, 1985). For actin labeling, F-actin (2.0 mg/ml; 0.1 M KCl, 0.6 mM ATP and 20 mM $NaHCO_3$) was mixed with 250 μM tetramethylrhodamine-5(and-6)-iodoacetoamide (Molecular Probes) and stored over night at 0°C. The solution was ultracentrifuged at 100,000 × *g* for 90 min, and the pellet was dissolved in 0.1 mM ATP, 10 mM MOPS (pH 7.0), 1.5 mM NaN_3, 1 mM DTT and 50 μM $CaCl_2$; the resulting solution was dialyzed against the same solvent at 2°C. After sufficiently depolymerizing the actin, the solution was ultracentrifuged again. Sephadex G25 (fine) was used for final removal of a trace amount of free dye. About 55% of actin was labeled. The critical concentration for polymerization of labeled actin was slightly higher than that of unlabeled actin.

Examination of actin binding to nebulin in myofibrils

To examine the binding of actin to the portion of nebulin that had been dissociated from actin filaments as a result of the gelsolin treatment of

myofibrils, fluorescence dye-labeled F-actin (0.5 mg/ml) was added to skeletal and cardiac myofibrils in a rigor (−Ca) solution containing 4 mM ADP. Free ATP in the F-actin solution was removed as much as possible by hydrolyzing it with 0.2 mg/ml hexokinase (Sigma Chemical Co., St. Louis, MO) in the presence of 1 mM glucose. Within 10 s to 10 min after the addition of actin to the myofibrils, unbound actin was washed out with a rigor (−Ca) solution and the region into which labeled F-actin had been incorporated was examined by fluorescence and phase-contrast microscopy.

RESULTS

Sarcomere structure in RG-treated and CG-treated myofibrils

First, we examined how thin filaments were removed in the RG-treated and CG-treated myofibrils. Thin filaments of about 1 μm in length were present at both sides of the Z line in an untreated myofibril (Fig. 1 *a*). After the gelsolin treatment in an RG-solution, only the portion of the thin filament located at the I band had been removed (note the dark I band in Fig. 1 *b*), whereas the portion of the thin filament located at the A band remained intact (note the width of each fluorescent band in the doublet located at the center of each sarcomere in Fig. 1 *b*; see also Discussion; cf. Funatsu et al., 1990); in addition, short fragments remained at the Z line. To examine this myofibril model, the solution was finally exchanged for a rigor (−Ca) solution and then for a relaxing solution for each purpose. The RG-treated myofibril was further treated with gelsolin in a CG-solution. As a result, thin filaments other than the fragments at the Z line were removed (note that only the Z line in the I-Z-I brush is fluorescent in Fig. 1 *c*). The solution was finally exchanged for a relaxing solution.

Second, we examined whether nebulin was exposed at the I band in the RG-treated myofibril. If exposed nebulin is present at the I band, exogenous F-actin may bind to that exposed portion, because *in vitro* experiments have shown that a part of nebulin molecule binds to F-actin (Jin and Wang, 1991; Chen et al., 1993; Pfuhl et al., 1994). Fig. 2 demonstrates the binding of rhodamine-labeled F-actin to the I band region of the RG-treated skeletal myofibril (Fig. 2 *a*). This binding did not occur in the RG-treated cardiac myofibril (Fig. 2 *b*). Fig. 2 *c* confirms that the portion of the thin filament located at the I band was selectively removed from cardiac myofibrils, as is essentially the case in skeletal myofibrils (cf. Fig. 1 *b*). Rhodamine-labeled G-actin did not bind to the RG-treated myofibrils under low salt, nonpolymerizable conditions (data not shown). On the other hand, such binding of F-actin was not observed in untreated myofibrils for either skeletal or cardiac muscles (data not shown; for skeletal myofibrils see Ishiwata and Funatsu, 1985). These results suggest that exposed nebulin is present in skeletal muscle after RG-treatment.

Third, we examined whether nebulin connects the Z line and the portion of the thin filament remaining as fragments at the A band in the RG-treated myofibril. If nebulin does form a connection, the thin filament fragments at the A band should move with extension of the sarcomere under relaxing conditions, whereas it would not be expected to move under rigor conditions. Fig. 3 *a–c* show that under rigor conditions, the bright doublets corresponding to the free ends of thin filaments observed on a fluorescence micrograph (Fig. 3, *b* and *c*) did not change their position when sarcomere length was extended from 2.76 μm (Fig. 3 *b*) to 3.06 μm

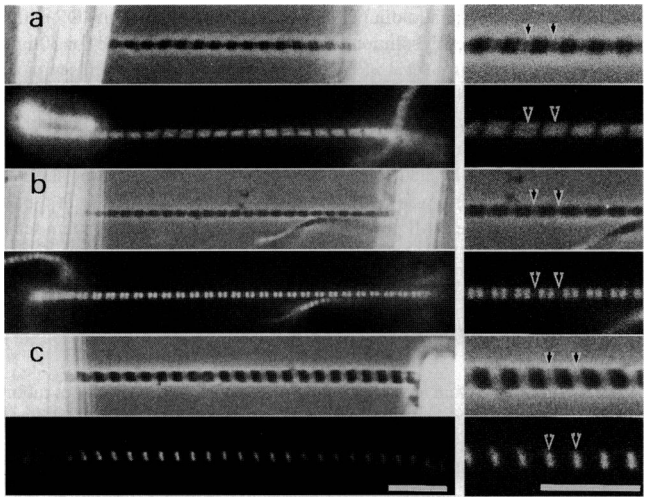

FIGURE 1 Optical micrographs of myofibrils before and after gelsolin treatment. Actin filaments were visualized by rhodamine-phalloidin staining after formaldehyde fixation. (*a*) Untreated myofibril; (*b*) myofibril treated with gelsolin in an RG-solution; (*c*) myofibril further treated with gelsolin in a CG-solution. All procedures were done at room temperature. The upper and lower parts of each figure are phase-contrast and fluorescence micrographs, respectively. Enlarged figures are shown on the right. The reason why the fluorescence intensity of the Z line in *c* looks much greater than that in *b* is that the exposure time to take the photograph of *c* was longer than that of *b*. Also, it is to be noted that the appearance of the A band in phase-contrast micrograph differs depending on the position of focal plane (cf. *b* and *c*). Arrows indicate the positions of the Z lines. Uniform sarcomere length (*L*) were maintained even after the gelsolin treatment and stretching of myofibrils (SD of *L* was less than 1% of the average *L* in the examples shown here). Scale bars, 10 μm.

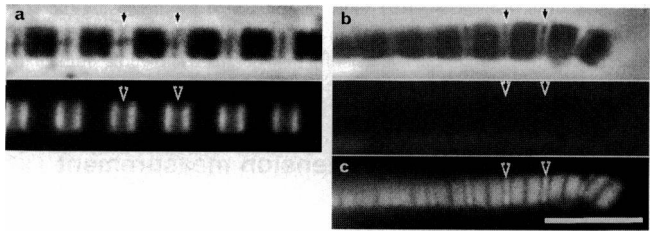

FIGURE 2 Optical micrographs of RG-treated myofibrils of skeletal and cardiac muscle. Rhodamine-labeled F-actin (0.5 mg/ml, without ATP) was added to an RG-treated myofibril of skeletal muscle (*a*) or cardiac muscle (*b*) in a rigor (−Ca) solution. As a reference, the RG-treated cardiac myofibril was stained with rhodamine phalloidin after formaldehyde fixation (*c*, the same myofibril as in *b*). The upper and lower parts of *a* and *b* are phase-contrast and fluorescence micrographs, respectively, and *c* is a fluorescence micrograph. All procedures were done under a microscope, without holding the ends of myofibrils, at room temperature. The I band width in the cardiac myofibril is small because the slack sarcomere length is short. The fluorescence pattern obtained in *a* was essentially the same even at shorter I band width. Arrows indicate the positions of the Z lines. Scale bar, 5 μm.

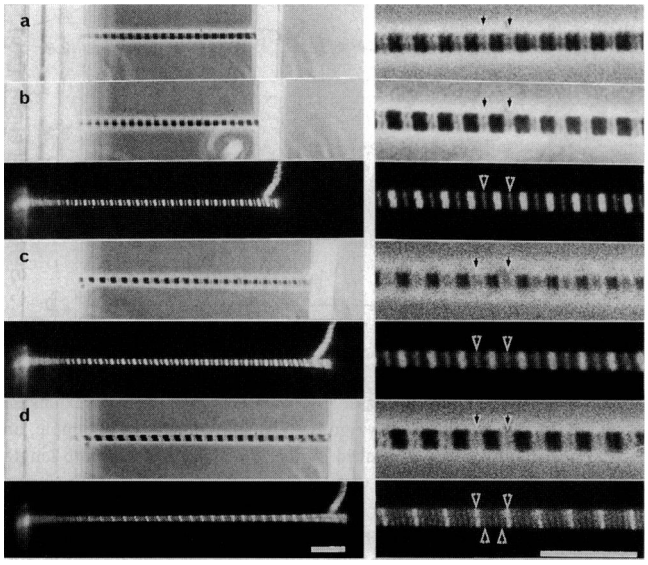

FIGURE 3 Optical micrographs showing the effects of extension on RG-treated myofibrils under rigor and relaxing conditions. The free ends of thin filaments and the Z line were visualized by rhodamine-phalloidin staining without formaldehyde fixation. (*a*) Untreated myofibril (average sarcomere length (*L*), 2.65 μm); (*b*) myofibril of *a* after gelsolin treatment in an RG-solution (*L*, 2.76 μm); (*c*) myofibril of *b* that had been stretched to an *L* of 3.06 μm in a rigor (−Ca) solution and then (*d*), the rigor (−Ca) solution was exchanged for a relaxing solution containing BDM (*L*, 3.14 μm). All procedures were done at room temperature. The upper and lower parts of each figure are phase-contrast and fluorescence micrographs, respectively. The fluorescence micrograph of *a* was omitted because it was essentially the same as that of *b*. Enlarged figures are shown on the right. Arrows pointing from the upper sides of myofibrils indicate the positions of the Z lines. Both the central fluorescent doublet (*b* and *c*) and the quartet (*d*) in each sarcomere correspond to the free ends of thin filaments. Arrows pointing from the lower side of the myofibril in *d* indicate the outer pair of quartet bands originating from the central doublet of *c*. Scale bars, 10 μm.

(Fig. 3 *c*). That is, the free ends of thin filaments did not move and only the I band was elongated.

The average separation between a pair of doublets across the Z line, i.e., the apparent length of the I-Z-I brush, increased from 2. 24 to 2.55 μm, suggesting that the I band had been elongated by 0.16 (=(2.55 − 2.24)/2)μm. On the other hand, the I band width was 0. 58 (=(2.76 − 1.6)/2) μm before extension and 0.73 (=(3.06 − 1.6)/2) μm after extension, where the A band width was assumed to be 1.6 μm. From these values, the extent of elongation of the I band was calculated to be 0.15 (= 0.73 − 0.58) μm, consistent with the above value, i.e., 0.16 μm. Because the sarcomere length was 2.65 μm and the I band width was 0.52 μm before RG-treatment (Fig. 3 *a*), the I band was stretched by about 40% (=(0.73 − 0.52)/0.52) all together after the RG-treatment.

Accompanying the exchange of the rigor solution for a relaxing one, the doublet bands (Fig. 3 *c*) were split into four, i.e., a quartet (Fig. 3 *d*); an inner pair of bands was located in the central portion, and an outer pair was located near the Z line (cf. *bottom arrows* in Fig. 3 *d*) in each sarcomere. The fluorescence intensity showed that the proportion of inner and outer bands was about 1. Fig. 3 *d* illustrates the attained sarcomere length of 3.14 μm, slightly longer than that shown in Fig. 3 *c*; the average separation between the inner bands across the Z line was 2.55 μm, nearly the same as that shown in Fig. 3 *c*, whereas the average separation between the outer bands across the Z line was 1.43 μm, much shorter than the above. The latter result strongly suggests that at least about half of the thin filament fragments remaining at the A band are connected to the Z line through an elastic body, probably nebulin, and that nebulin shrinks as cross-bridges are detached in a relaxed state in the presence of BDM. We noticed that the outer pair of bands could not be observed in the relaxing solution without BDM, suggesting that at room temperature a small number of cross-bridges were still attached.

We interpret the above results as summarized schematically in Fig. 4. The fine structures of sarcomeres in RG-treated (cf. Figs. 1 *b* and 3, *b* and *c*) and CG-treated (Fig. 1 *c*) myofibrils correspond to those shown in Fig. 4, *b*, *c*, and *e*, respectively (for further detail, see Discussion). Under rigor conditions, the portions of thin filaments located at the A band remain intact as fragments maintaining rigor cross-bridges (Fig. 4 *b*). On stretching of the RG-treated myofibril, only the I band is elongated (Fig. 4 *c*). Accompanying re-

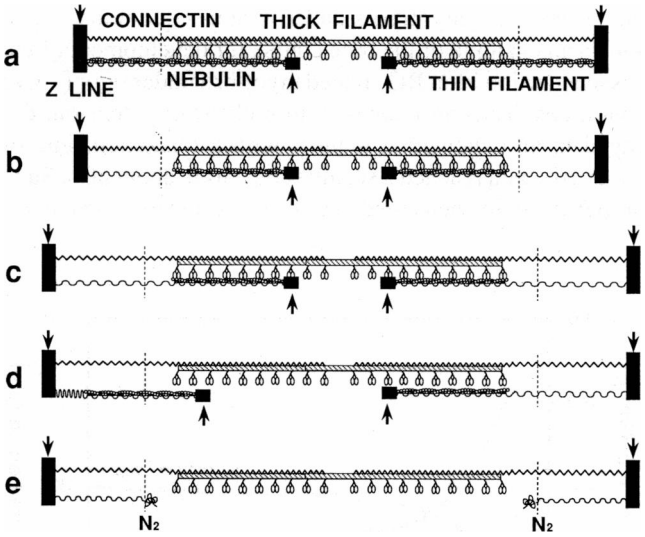

FIGURE 4 Schematic illustration showing the assumed filament structure of a sarcomere before and after gelsolin treatment. (*a*) Untreated sarcomere before gelsolin treatment; the fine structures of thick and thin filaments together with connectin (titin) and nebulin are depicted schematically. (*b* and *c*) RG-treated sarcomere under rigor conditions; because of the gelsolin treatment in an RG-solution, the portions of thin filaments located at the I band have been removed, so that a portion of each nebulin molecule is expected to be exposed (*b*) and with sarcomere stretching (*c*) only the I band is elongated without movement of the thin filament fragments remaining at the A band. (*d*) RG-treated sarcomere under relaxing conditions; the remaining fragments of thin filaments move to the Z line (*left* half) or stay as in *c* (*right* half) depending on whether the exposed portion of the nebulin molecule shinks. (*e*) CG-treated sarcomere; thin filaments are removed by further treatment of *c* with gelsolin under contracting conditions, so that the nebulin is free of actin filaments. Portions of the free ends of nebulin appear to be folded and have become entangled at the N_2 line (cf. Funatsu et al., 1990). Dashed lines indicate the approximate position of the N_2 line. Arrows indicate the position at which rhodamine-phalloidin staining occurs without chemical fixation.

laxation, as illustrated in the left half of Fig. 4 *d*, a portion of the thin filament fragments moves to the Z line, forming the outer pair of fluorescent bands (cf. Fig. 3 *d*); another portion barely moves at all, as illustrated in the right half of Fig. 4 *d*, forming the inner pair of fluorescent bands (cf. Fig. 3 *d*).

Here we present another piece of data consistent with the above structure of the gelsolin-treated sarcomere illustrated in Fig. 4. Fig. 5 is an example showing the time course of the tension development in an RG-treated myofibril that occurred as a result of CG-treatment. The active tension developed at the initial peak was nearly one-tenth of the tension developed under normal contracting condition with Ca^{2+}. This degree of active tension could not be eliminated even when the RG-treatment was prolonged; the exposed nebulin connecting the thin filament fragment and the Z line is considered to be responsible for the transmission of this active tension generation.

Time course of tension development with the extension of RG-treated myofibrils and viscoelastic analysis

We measured the tension passively developed accompanying the extension of myofibrils under various conditions. Fig. 6 shows an example of the time course for development of the passive tension in an RG-treated myofibril under rigor (−Ca) conditions. Tension increased abruptly with extension, decayed in an exponential manner with a relaxation time of about 10 s, and reached a steady state within about 60 s. Such properties were unchanged in CG-treated and untreated myofibrils under relaxing conditions, although the relaxation times were different. On the other hand, the tension response in an untreated myofibril under rigor conditions immediately reached a steady state without decay (data not shown).

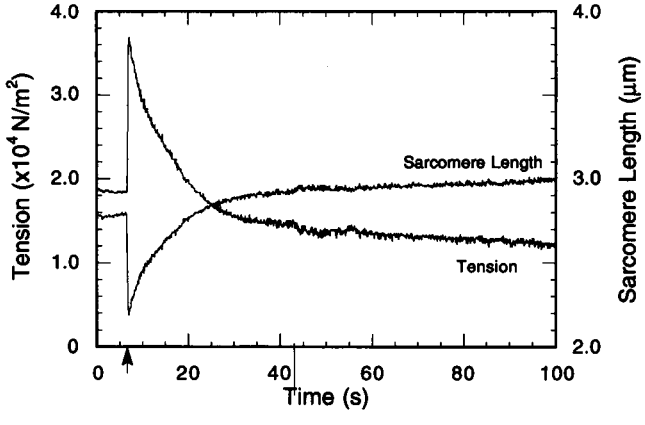

FIGURE 5 Time course of active tension development and sarcomere length change in an RG-treated myofibril accompanying CG-treatment. First, the myofibril treated with RG-solution at an average sarcomere length of 2.47 μm was stretched to 2.79 μm, so that the rigor tension was developed. Then, the solution was exchanged for CG-solution (see *arrow*). Active tension developed quickly increasing from 1.86×10^4 N/m² to a peak of 3.71×10^4 N/m²(sarcomere length, 2.2 μm) within 0.6 s. After the tension had risen to the peak level, it decreased exponentially to a level of 1.4×10^4 N/m² (sarcomere length, 3.0 μm). The myofibril used here is the same as that shown in Fig. 7. In this case, no feedback control was used, so that the myofibril length changed in accordance with the tension change. Hooke's elastic constant of the flexible glass micro-needle was 0.57 μg/μm.

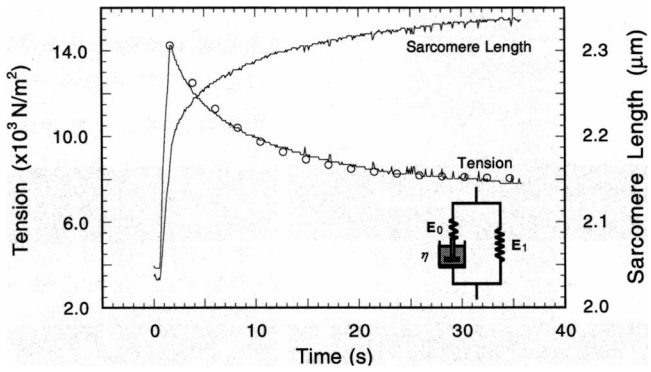

FIGURE 6 Time course of passive tension development with extension of an RG-treated myofibril in a rigor (−Ca) solution. In this example, an RG-treated myofibril was stretched so that the average sarcomere length quickly changed from 2.03 μm to 2.19 μm together with a tension change from 3.8×10^3 N/m² to 14.3×10^3 N/m². When the tension had decreased to a steady level, the average sarcomere length was 2.33 μm; the steady tension at this sarcomere length, 7.8×10^3 N/m², has been plotted in Fig. 7. The ordinate, tension (N) per unit cross section (m²) of myofibrils of which the cross sectional area (1.8×10^{-12} m²) was estimated from the average width of a myofibril assuming a circular cross section. Hooke's elastic constant of the flexible glass micro-needle was 0.22 μg/μm. (*inset*) Visco-elastic model representing each half sarcomere used for describing the time course of tension decay, which is composed of two Hookean springs (E_0 and E_1) connected in parallel and a viscous element (η) connected to a spring (E_0) in series. A best-fit result is superimposed on the experimental result with open circles.

We estimated the elastic modulus of nebulin based on the assumption that a viscoelastic model composed of viscous and elastic elements shown in the insert of Fig. 6 represents each half sarcomere; at this sarcomere length, shorter than 2.5 μm, the contribution of connectin (titin) is considered to be negligible (see Discussion). The time course of tension decay after stretch is described as follows:

$$\frac{(\text{passive tension})}{S}\ (\text{in units of N/m}^2) = \frac{\dfrac{E_1 \cdot X_0}{n}}{1 + \dfrac{E_1 \cdot S}{n \cdot k}} + \frac{\dfrac{E_0 \cdot X_0}{n}}{\left(1 + \dfrac{(E_0 + E_1) \cdot S}{n \cdot k}\right) \cdot \left(1 + \dfrac{E_1 \cdot S}{n \cdot k}\right)} \cdot \exp\left[- \frac{1 + \dfrac{E_1 \cdot S}{n \cdot k}}{1 + \dfrac{(E_0 + E_1) \cdot S}{n \cdot k}} \cdot \frac{E_0}{\eta} \cdot t \right], \quad (1)$$

where S is the cross sectional area of myofibril, X_0 is the displacement of the rigid micro-needle, E_0 and E_1 are (elastic moduli)/S, η is (a viscous coefficient of dashpot)/S, n is a number of half-sarcomeres connecting in series in the myofibril, and k is Hooke's elastic constant of the flexible micro-

needle. The values of E_1 and E_0 were estimated from the final plateau level and initial peak of tension, respectively, whereas the value of η was estimated from the decay rate (cf. Fig. 6). The best result was obtained in Fig. 6 by setting the values of E_0, E_1, and η at 2.8×10^4 N/m^2, 5.7×10^3 N/m^2, and 2.3×10^5 N · s/m^2, respectively.

If the cross sectional area per a single thin filament of a myofibril is assumed to be 7×10^{-16} m^2 (center-to-center distance between thick filaments, 40 nm), the E_0, E_1, and η values per thin filament are estimated to be 20 pN, 4.0 pN, and 17 pN · s, respectively. If two nebulin molecules are bound to one thin filament (this is still speculative), the values of these parameters for a single nebulin molecule become half of the above values.

Tension versus extension relation of myofibrils under various conditions

Passive tension development was examined with stepwise stretching of myofibrils under various conditions. Fig. 7 depicts typical examples of tension versus extension relations for an untreated myofibril under rigor (−Ca) and relaxing conditions (±BDM), for an RG-treated myofibril under rigor (−Ca) conditions and for a CG-treated myofibril under relaxing conditions (−BDM). A steady level of tension was measured after stepwise stretching of myofibrils starting from a slack sarcomere length to longer sarcomere lengths plotted on the abscissa. As shown in Fig. 7, the developed passive tension of untreated myofibrils in a relaxing solution containing 20 mM BDM was smaller than that observed in the absence of BDM. This suggests that some fraction of the cross-bridges were still attached in the relaxing solution without BDM at room temperature.

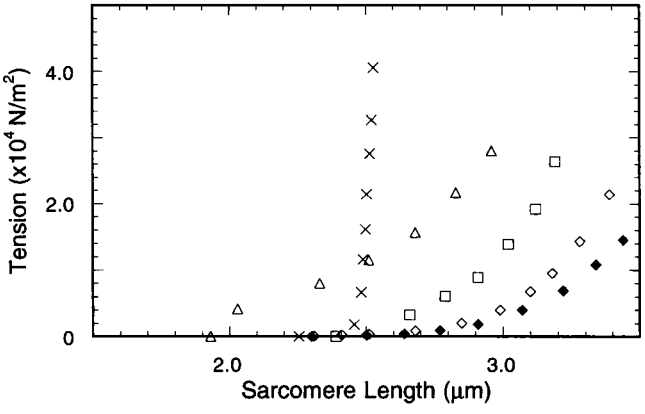

FIGURE 7 Passive tension versus extension relation of myofibrils under various conditions before and after gelsolin treatment (cf. Figs. 1, 3, and 4). First, an untreated myofibril at an average sarcomere length of 2.47 μm (L_0) was gradually extended in a rigor (−Ca) solution, and the tension was measured (×); after returning to the initial sarcomere length (L_0), it was treated with gelsolin in a rigor (+Ca) solution (RG-treated myofibril; cf. Figs. 1, 3, and 4), and the passive tension was measured stepwise (△) in a rigor (−Ca) solution starting from a slack length at which there was no tension, L_R (about 1.93 μm in this case); the RG-treated myofibril was further treated with gelsolin in a contracting solution after returning to L_0 (CG-treated myofibril; cf. Figs. 1, 3, and 4) and the passive tension was measured stepwise (□) in a relaxing solution without BDM starting from a slack length, L_S (about 2.38 μm in this case). As a control, the passive tension of an untreated myofibril was also measured in a relaxing solution without (◇) and with (◆) BDM by using a different specimen. The tension at a steady state (cf. Fig. 6) was plotted at each sarcomere length (L) after the extension.

The shape of almost all curves was concave except in RG-treated myofibrils, for which the curve was convex at shorter sarcomere length. The slack sarcomere length, at which the tension disappears, was shortest in an RG-treated myofibril (L_R). Tension developed spontaneously as a consequence of RG-treatment, suggesting that an elastic body, probably nebulin, shrinks in response to removal of the portion of the thin filament located at the I band. This is consistent with the formation of the outer fluorescent doublet in the quartet, as described in Fig. 3 *d* (see Discussion).

After complete removal of the thin filaments by CG-treatment, the tension versus extension relation became concave and resembled that of an intact myofibril under relaxing conditions. This result is consistent with a previous result obtained using a single muscle fiber (Funatsu et al., 1990). A slight difference between the present and previous results is that greater tension development was observed in this study, although the extent of the shift in slack length (L_S) to the left (from about 2.5 to 2.4 μm in this example) was similar. The difference became larger as the transient tension development and the shortening of sarcomeres were increased with CG-treatment (cf. Fig. 5). To minimize this effect, shortening of myofibrils was suppressed to some extent by feedback control with a piezo element when the solution was exchanged from an RG-solution to a CG-solution.

Tension versus extension relation of an RG-treated myofibril

To study the elastic properties of nebulin of various lengths, RG-treated myofibrils were prepared under different conditions of sarcomere length (L_0). The use of this procedure allows the length of the exposed portion of nebulin to be controlled according to the assumed filament structure of the RG-treated myofibril (cf. Fig. 4, *b* and *c*). The length of the exposed portion of nebulin was estimated by $(L_0 - L_A)/2$, where L_A is an A band width (cf. Fig. 4). Fig. 8 *a* shows five examples thus obtained, corresponding to five different L_0 (indicated by *arrows*), i.e., 2.25, 2.31, 2.47 (the same as in Fig. 7), 2.47, and 2.72 μm, and the slack lengths (L_R) were 1.76, 1.90, 1.93 (the same as in Fig. 7), 1.98, and 2.11 μm, respectively. The data were reproducible within this range of sarcomere lengths (L) less than 3.2 μm.

The relative tension versus extension relation was replotted against the assumed natural length of the exposed portion of nebulin, i.e., $(L_R - L_A)/2$, at which length the stress of nebulin is expected to disappear. The results summarized in Fig. 8 *b* show that all relations, except at large λ, overlap with each other; the overlapping region was extended if the contribution of resting tension, which appeared at $L > 2.5$ μm (cf. Fig. 7), was simply subtracted.

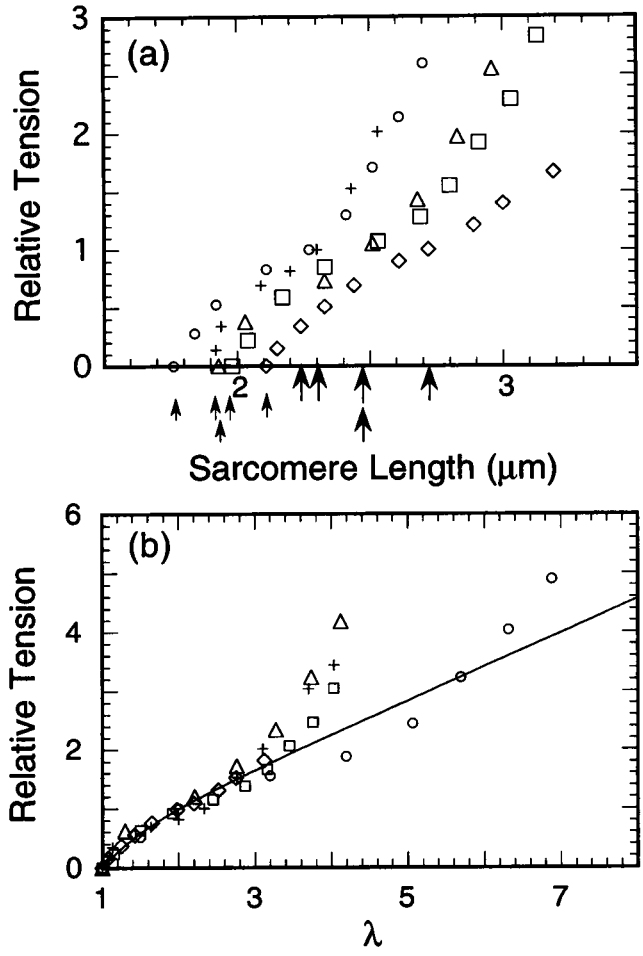

FIGURE 8 Passive tension versus extension relation of RG-treated myofibrils in a rigor (−Ca) solution. (*a*) RG-treated myofibrils (cf. Figs. 1, 3, and 4) were prepared at average sarcomere length (L_0) of 2.25 (○), 2.31 (+), 2.47 (△, □), and 2.72 (◇) μm, as indicated by the large arrows. (△) A replot of Fig. 7. Relative tension was obtained by normalizing the tension against that developed at the initial sarcomere length (L_0) at which the gelsolin treatment was done. Measurement procedures, the same as in Fig. 7. (*b*), in the relative tension versus extension relation obtained in *a*, the sarcomere length was first replotted against $(L - L_A)/(L_R - L_A) = \lambda$, where L is a variable sarcomere length, L_A a thick filament length (assumed to be 1.6 μm) and L_R is the slack sarcomere length, which differs among myofibrils as indicated by small arrows (1.76 (○), 1.90 (+), 1.93 (△), 1.98 (□), and 2.11 (◇) μm); each tension curve was further normalized by the relative tension at $\lambda = 2$. A thin line represents $(4/7)(\lambda - 1/\lambda^2)$, a normalized equation describing rubber elasticity.

Homogeneity and constancy of sarcomeres during extension

Fig. 9 is an example of an image profile from phase-contrast micrograph of an untreated myofibril (Fig. 9 *a*), an RG-treated myofibril (Fig. 9 *b–d*), and a CG-treated myofibril (Fig. 9 *e*). Neither over-stretched nor over-shortened sarcomeres could be observed. In this example, the SD of sarcomere lengths in each myofibril was about 2% of the average sarcomere length (cf. in an example shown in Fig. 1, SD was less than 1%). This sarcomere homogeneity was maintained throughout the present experiments.

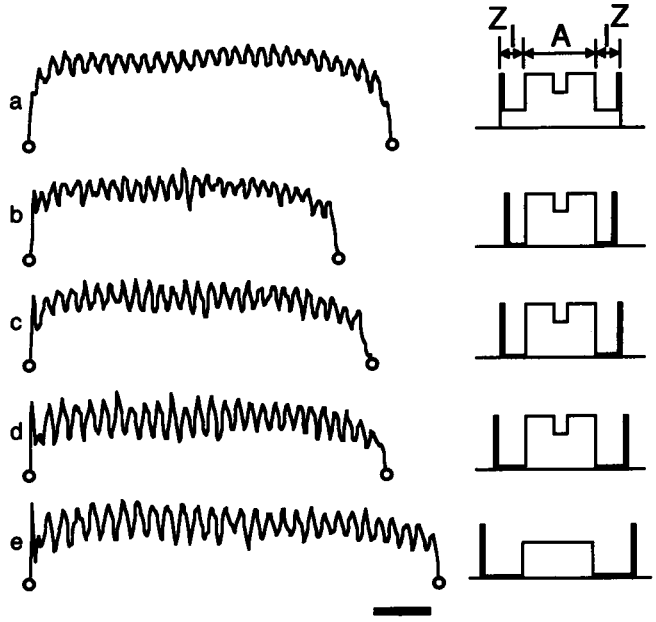

FIGURE 9 Image profile of a myofibril obtained by phase-contrast microscopy. The horizontal and vertical axes represent the position along a myofibril and darkness of the phase-contrast image, respectively. The two circles on either side correspond to the inner edges of the micro-needles. A peak and a valley of the image profile correspond to the center of the A band and the Z line, respectively (the Z line is not clear because of the low resolving power of the objective lens used here (Plan 60 × DM, Nikon)); the density profile of each sarcomere is schematically illustrated at the right-hand side. (*a*) Untreated myofibril in a rigor (−Ca) solution (L (average sarcomere length) = 2.50 μm); (*b–d*), the RG-treated myofibril was stretched stepwise in a rigor (−Ca) solution (L = 2.24 (*b*), 2.46 (*c*), and 2.69 (*d*) μm; SD of L was at most 2% of L); (*e*) the CG-treated myofibril in a relaxing solution (L = 3.16 μm; the number of sarcomeres, 29). Here, we have shown an example in which the number of sarcomeres between the inner edges of micro-needles increased from 25 to 27 on extension of a myofibril; when firmly adhering to a glass surface, the number of sarcomeres did not change. For phase-contrast images and conditions, see Figs. 1 and 3. Scale bar, 10 μm.

DISCUSSION

Have we really succeeded in measuring the elastic modulus of nebulin?

The validity of the present work, especially the estimation of elastic modulus of nebulin, relies upon the assumption that a certain portion of nebulin is exposed in a manner such as that illustrated in Fig. 4 *b* after RG-treatment and that this exposed portion of nebulin is most compliant in the RG-treated myofibril. Our results provide evidence supporting this assumption. First, as Fig. 1 *b* demonstrates, the portion of the thin filament located at the I band was selectively removed; on the other hand, the portion of the thin filament located at the A band remained as fragment. Judging from the fluorescence intensity of the rhodamine phalloidin-labeled RG-treated myofibril (Fig. 1), actin filaments remaining at the I band were negligibly few in number. Even if actin filaments remained after the gelsolin treatment, they would have been destroyed by such massive extension, i.e.,

by several tens of % (cf. Figs. 3 and 7–9) because actin filaments are not sufficiently extensible so as to be capable of enduring a stretch of more than 10% (cf. Kishino and Yanagida, 1988). The possibility of persisting tropomyosin threads is also small, because tropomyosin and troponin actually diffuse out of muscle fibers (cf. Funatsu et al., 1990).

Furthermore, exogenous F-actin attached to the I band in skeletal muscle after RG-treatment, whereas it did not in cardiac muscle in which nebulin is absent (Fig. 2). We confirmed as previously reported, as a control, that in an untreated muscle exogenous F-actin did not bind to the I band (cf. Ishiwata and Funatsu, 1985). The nebulin molecule is now considered to be located along an actin filament, in a side-by-side fashion, over its entire region from the free end of a thin filament to the Z line (cf. Wang and Wright, 1988; Wright et al., 1993). It is thus probable that the portion of nebulin located at the I band was dissociated from an actin filament and thereby exposed.

A third piece of evidence supporting our assumption that the actual elasticity of nebulin was measured is that only the I band was uniformly elongated on stretching RG-treated myofibrils (cf. Figs. 3 *c* and 9 *b–d*). This indicates that the I band is the most extensible (compliant) component of a gelsolin-treated sarcomere structure, such that the elastic modulus estimated herein can be ascribed primarily to the elastic structure located at the I band.

Fourth, the mechanical connection between the thin filament fragments that remained at the A band and the Z line was demonstrated by the following results. (1) An atypical tension versus extension relation, especially in regards to tension development, was obtained under rigor conditions for RG-treated myofibrils at the sarcomere lengths at which the gelsolin treatment was done and, in addition, where the contribution of connectin (titin) was negligibly small because of the reason discussed below and judging from the fact that the slack sarcomere length of untreated and CG-treated myofibrils is about 2.5 μm (Fig. 7) longer than that of RG-treated ones (Fig. 8 *a*). (2) Active tension, nearly one-tenth of the tension obtained under normal contracting condition, was produced transiently in association with CG-treatment of RG-treated myofibrils (Fig. 5). There is no possibility that 10% of the thin filaments were intact at that point because the I band was elongated by 40% under rigor conditions before the CG-treatment as described above.

Fifth, as shown in Fig. 3, although the fluorescent doublets that represent the free ends of the thin filament fragments did not move with stretching of the sarcomere in a rigor solution, about a half of them did move to the Z line as soon as the solution was exchanged for a relaxing one containing BDM. The distance between the outer fluorescent band and the Z line observed in Fig. 3 *d* (1.43/2 μm) just corresponded to (the length of the thin filament fragments remaining at the A band (about 0.5 μm)) + (the assumed natural length of the exposed portion of the nebulin (about 0.2 μm; cf. Fig. 8) at a sarcomere length of 2.65 μm). This correspondence strongly suggests that the exposed portion of the nebulin shrinks to its assumed natural length.

Sixth and finally, we should examine a possibility that the exposed portion of nebulin is entangled with the elastic filaments in the RG-treated myofibrils. The passive tension versus extension relation shown in Figs. 7 and 8 may be explained by assuming that the exposed portion of nebulin is collapsed onto a portion of connectin (titin) filaments so as to make it shorter and nonextensible. As a result of the shortened length of the extensible segment, the slack sarcomere length may shift toward the shorter one. But, because the entanglement is not considered to be released by the CG-treatment, the shortened slack length should remain unchanged after the CG-treatment. Fig. 7 shows that this is not the case.

Alternatively, there remains a possibility that the exposed portions of nebulin themselves are entangled with each other in the RG-treated myofibrils. In this case, the shortened slack length may be reversibly returned to the original length after the CG-treatment, because all of the thin filament fragments remaining at the A band are removed by the CG-treatment (cf. Fig. 4 *e*). If such entanglement occurs, the value we estimated puts an upper limit on the elastic modulus of nebulin.

Thus, we conclude that the elastic properties of the exposed portion of nebulin could be studied under a situation such as that illustrated in Fig. 4 *b*.

At present, it is important to ascertain what proportion of nebulin was preserved intact after the gelsolin treatment. First, we can point out that our previous SDS-PAGE studies on single muscle fibers showed that at most 25% of nebulin was removed, probably by proteolysis, leaving more than 75% of nebulin intact, after the CG-treatment (see Fig. 1 in Funatsu et al., 1990, 1993). The duration of gelsolin treatment was much shorter in the present study than that utilized in the previous studies, although the temperature was higher. There is a report showing that nebulin is fragmented by 0.1 mM Ca^{2+} (Tatsumi and Takahashi, 1992), but this effect can be neglected, because nebulin from the rabbit psoas muscle is reported to be stable for up to one day of incubation and the duration of Ca^{2+} incubation in the present study was short (less than 1 h in total).

Even if nebulin was not digested by proteolysis, the possibility remains that one end of the nebulin molecule was detached from the Z line. We estimate that at least half of the thin filament fragments located at the A band are mechanically attached to the Z line through the exposed portion of nebulin, based on the fluorescence intensity distribution of the quartet shown in Fig. 3 *d*.

Thus, although there is a possibility that the elastic modulus of nebulin given in Results is an underestimate, the extent of underestimation being within a 10-fold limit even when two to three factors of overestimation of the cross sectional area of a myofibril are taken into account.

Contribution of nebulin to the elasticity of thin filaments

If nebulin attaches to a thin filament only at the free end of the thin filament and the Z line, the entire length of nebulin will be extended even in RG-treated myofibrils irrespective of the extent of thin filament removal, so that the slack length (L_R) should be independent of the length of the portion of the thin filaments removed. The fact that L_R decreased with the decrease in L_0 (Fig. 8 *a*) suggests that nebulin is attached to an actin filament in a side-by-side fashion between about 0.3 and 0.6 μm from the Z line. Also, the fact that the convex curves obtained at different L_0 overlapped each other after normalization (Fig. 8 *b*) suggests that the exposed portion of nebulin is mechanically uniform, at least, at the I band region we examined (up to 0.6 μm from the Z line).

The static elastic modulus, E_1, of the exposed portion of nebulin, i.e., E_1 per thin filament, was also estimated from the slope of the tension versus extension relation at L_0 (before normalization in Fig. 8 *a*) to be 10.3 ± 7.6 (SD for $n = 5$) pN (=(10.3 ± 7.6) × 10^{-3} pN/nm for the 1 μm long exposed portion of nebulin); this value was essentially the same as the E_1 (4.0 pN) obtained in Fig. 6. Thus, the static elastic modulus of the exposed portion of nebulin is apparently 2 × 10^3 times smaller than that of an actin filament, which is estimated to be about 2 × 10^4 pN (=20 pN/nm for an actin filament 1 μm long and 2 nm in the effective radius of cross section) (cf. Fujime, 1987; Higuchi et al., 1993). If we take into account the possibility that the elastic modulus of nebulin thus obtained is a 10-fold underestimate, as considered above, the actual elastic modulus of nebulin should be 10 times larger than that estimated here. It is still, however, 2 × 10^2 times smaller than that of an actin filament. Thus, we conclude that nebulin, at least the portion of the molecule located within about 0.6 μm of the Z line, does not contribute to the static elastic modulus of thin filaments in muscle.

This conclusion may raise questions because the amino acid sequence suggests that nebulin is composed of an α-helix (Labeit et al., 1991; Pfuhl et al., 1994) and the elastic modulus of a single α-helix is estimated to be 2 × 10^3 pN (=2 pN/nm for α-helix (PBLG) 1 μm long; cf. Higuchi et al., 1993), several tens times larger than that estimated for nebulin in the present work. If nebulin is composed entirely of α-helix, such a low stiffness would not be expected. Our results suggest that nebulin is not composed entirely of α-helix.

Possible reasons for the convex relation between tension and extension in RG-treated myofibrils

There are at least two plausible quantitative explanations for the convex tension (K) versus extension relation obtained in RG-treated myofibrils (Figs. 7 and 8): (1) rubber elasticity due to cross-link formation among elastic filaments, and (2) a conformational change of nebulin between two states having different equilibrium length.

First, the curve can be partly simulated by an equation describing the rubber elasticity: $K = C(\lambda - 1/\lambda^2)$, where C is a constant containing an absolute temperature and λ is the relative degree of extension defined in Fig. 8. As shown by the master curve depicted in Fig. 8 *b*, the initial monotonous rising phase of the curves ($\lambda < 3$) can be simulated by the above equation taking C as 1.0 × 10^3 (*open circles*), 6.3 × 10^3 (*crosses*), 4.3 × 10^3 (*triangles*), 2.9 × 10^3 (*squares*), and 1.3 × 10^4 (*diamonds*) (N/m^2). The rubber elasticity requires cross-linking among elastic filaments and a constant myofibril volume. This appears to be analogous to a model of connectin (titin) configuration in cardiac muscle suggested by Funatsu et al. (1993). However, in the above discussion, we have excluded a possibility that exposed portion of nebulin gets entangled in connectin (titin) in the RG-treated myofibrils. Therefore, in the future, we should examine another possibility that the exposed portions of nebulin themselves are entangled with each other.

Second, the convex curve was similar to that obtained for wool (Speakman, 1927). Therefore, an alternative explanation would be that nebulin is composed of many structural units, each of which can exist in two states having different equilibrium lengths. When released from actin filaments, a structural unit with a shorter equilibrium length is assumed to be more stable than a longer one, so that extra tension appears spontaneously at L_0. A comparable idea was successfully applied to keratin molecules (for experimental work, cf. Astbury and Woods, 1933; for a theoretical model, cf. Kubo, 1965). The theoretical model was recently adopted by Oda and Go to explain the elastic properties of connectin (titin) (Oda and Go, 1992). It can simulate exactly the curve obtained for an RG-treated myofibril (Fig. 8) over its entire length (even $\lambda > 3$) if appropriate parameter values are selected (cf. Fig. 7 in Oda (1993)). This explanation is consistent with the assumed filament structure illustrated in Fig. 4, *c* and *d*. To clarify this problem, the fine structure of exposed nebulin at its natural and slack length should be determined in the future.

Resting tension and elastic properties of connectin (titin)

In the present study, we confirmed a previous result indicating that the tension versus extension relation of CG-treated single fibers is similar to the resting tension versus extension relation of intact fibers (Funatsu et al., 1990). The absolute value of resting tension itself was similar to that obtained in previous studies; e.g., 1.4 × 10^4 N/m^2 at $L = 3.4$ μm in an example shown in Fig. 7 (cf. Moss and Halpern, 1977; Magid et al., 1984; Magid and Law, 1985; Bartoo et al., 1993). Compared with our previous results (compare Fig. 7 with Fig. 7 in Funatsu et al., 1990), the curve shifted to the upper left-hand side in the CG-treated myofibrils. This can probably be ascribed to a certain degree of damage, e.g., entanglement of the filaments produced in the lattice structure due to the shortening of, or active tension development in, sarcomeres during CG-treatment. Preliminary experiments showed that this transient shortening could be partially suppressed by the addition of BDM maintaining the isomet-

ric length of myofibrils, but it was difficult to suppress contraction completely at room temperature (lowering the temperature, however, is effective). Such damage may have been minimized in the fiber, because the gelsolin treatment was done at 2°C. In this respect, Takemori's (1991) observation that the resting tension of a skinned semitendinosus frog muscle increased gradually with contraction may be relevant, although he did not indicate clearly why this occurred.

The above situation may be clarified if we use cardiac muscle in which nebulin is absent; but, unfortunately, we have not yet succeeded in manipulating a cardiac myofibril using the same technique as that applied to a skeletal myofibril. In any case, however, we can conclude that resting tension is attributable primarily to connectin (titin) filaments, as previously reported (Funatsu et al., 1990).

We thank Prof. S. Fujime of Yokohama City University for valuable advice and critical reading of an early version of this article.

This work was supported in part by grants-in Aid for Scientific Research (No. 04402053 to S. Ishiwata) and for Scientific Research on Priority Areas (No. 04237228 and 05221234 to S. Ishiwata) from the Ministry of Education, Science and Culture of Japan.

REFERENCES

Anazawa, T., K. Yasuda, and S. Ishiwata. 1992. Spontaneous oscillation of tension and sarcomere length in skeletal myofibrils. Microscopic measurement and analysis. *Biophys. J.* 61:1099–1108.

Astbury, W. T., and H. J. Woods. 1993. X-ray studies of the structure of hair, wool, and related fibers. II. The molecular structure and elastic properties of hair keratin. *Phil. Trans.* 232:333–394.

Bartoo, M. L., V. I. Popov, L. A. Fearn, and G. H. Pollack. 1993. Active tension generation in isolated skeletal myofibrils. *J. Muscle Res. Cell Motil.* 14:498–510.

Chen, M.-J. G., Shih C.-L., and K. Wang. 1993. Nebulin as an Actin Zipper. A two-module nebulin fragment promotes actin nucleation and stabilizes actin filaments. *J. Biol. Chem.* 268:20327–20334.

Ebashi, S. 1991. Excitation-contraction coupling and the mechanism of muscle contraction. *Annu. Rev. Physiol.* 53:1–16.

Fujime, S. 1987. Sarcomeric element flexibility. *In* Optical Studies of Muscle Cross-bridges. R. J. Baskin and Y. Yeh, editors. CRC Press, FL. 149–188.

Funatsu, T., H. Higuchi, and S. Ishiwata. 1990. Elastic filament in skeletal muscle revealed by selective removal of thin filaments with plasma gelsolin. *J. Cell Biol.* 110:53–62.

Funatsu, T., E. Kono, H. Higuchi, S. Kimura, S. Ishiwata, T. Yoshioka, K. Maruyama, and S. Tsukita. 1993. Elastic filaments in situ in cardiac muscle: deep-etch replica analysis in combination with selective removal of actin and myosin filaments. *J. Cell Biol.* 120:711–724.

Granzier, H. L. M., and K. Wang. 1993. Passive tension and stiffness of vertebrate skeletal and insect flight muscles: the contribution of weak cross-bridges and elastic filaments. *Biophys. J.* 65:2141–2159.

Harris, H. E., and A. G. Weeds. 1984. Plasma gelsolin caps and severs actin filaments. *FEBS Lett.* 177:184–188.

Higuchi, H., Y. Nakauchi, K. Maruyama, and S. Fujime. 1993. Characterization of β-connectin (titin 2) from striated muscle by dynamic light scattering. *Biophys. J.* 65:1906–1915.

Horowits, R., and R. J. Podolsky. 1987. The positional stability of thick filaments in activated skeletal muscle depends on sarcomere length: evidence for the role of titin filaments. *J. Cell Biol.* 105:2217–2223.

Ishiwata, S., T. Anazawa, T. Fujita, N. Fukuda, H. Shimizu, and K. Yasuda. 1993. Spontaneous tension oscillation (SPOC) of muscle fibers and myofibrils. Minimum requirements for SPOC. *In* Mechanism of Myofilament Sliding in Muscle Contraction. H. Sugi and G. H. Pollack, editors. Plenum Publishing Corp., New York. 545–556.

Ishiwata, S., and T. Funatsu. 1985. Does actin bind to the ends of thin filaments in skeletal muscle? *J. Cell Biol.* 100:282–291.

Jin, J.-P., and K. Wang. 1991. Nebulin as a giant actin-binding template protein in skeletal muscle sarcomere: interaction of actin and cloned human nebulin fragments. *FEBS Lett.* 281:93–96.

Kishino, A., and T. Yanagida. 1988. Force measurements by micromanipulation of a single actin filament by glass needles. *Nature.* 334:74–76.

Kruger, M., J. Wright, and K. Wang. 1991. Nebulin as a length regulator of thin filaments of vertebrate skeletal muscles: correlation of thin filament length, nebulin size, and epitope profile. *J. Cell Biol.* 115:97–107.

Kubo, R. 1965. Statistical mechanics. An Advanced Course with Problems and Solutions. North-Holland, Amsterdam. 134 and 153–155.

Kurokawa, H., W. Fujii, K. Ohmi, T. Sakurai, and Y. Nonomura. 1990. Simple and rapid purification of brevin. *Biochem. Biophys. Res. Commun.* 168:451–457.

Labeit, S., T. Gibson, A. Kakey, K. Leonard, M. Zeviani, P. Knight, J. Wardale, and J. Trinick. 1991. Evidence that nebulin is a protein-ruler in muscle thin filaments. *FEBS Lett.* 282:313–316.

Magid, A., and D. J. Law. 1985. Myofibrils bear most of the resting tension in frog skeletal muscle. *Science.* 230:1280–1282.

Magid, A., H. P. Ting-Beall, M. Carvell, T. Kontis, and C. Lucaveche. 1984. Connecting filaments, core filaments, and side-struts: a proposal to add thee new load-bearing structures to the sliding filament model. *In* Contractile Mechanics in Muscle. G. Pollack and H. Sugi, editors. Plenum Publishing Corp., New York. 307–328.

Maruyama, K. 1986. Connectin, an elastic filamentous protein of striated muscle. *Int. Rev. Cytol.* 104:81–114.

Maruyama K., A. Matsuno, H. Higuchi, S. Shimaoka, S. Kimura, and T.Shimizu.1989. Behavior of connectin (titin) and nebulin in skinned muscle fibers released after extreme stretch as revealed by immunoelectron microscopy. *J. Muscle Res. Cell Motil.* 10: 350–359.

Moss, R. L., and W. Halpern. 1977. Elastic and viscous properties of resting frog skeletal muscle. *Biophys. J.* 17:213–228.

Natori, R. 1954. The property and contraction process of isolated myofibrils. *Jikeikai Med. J.* 1:119–126.

Nave, R., D. O. Fürst, and K. Weber. 1990. Interaction of α-actinin and nebulin in vitro: support for the existence of a fourth filament system in skeletal muscle. *FEBS Lett.* 269:163–166.

Oda, K. 1993. A model for generation of resting tension in connectin. Master's dissertation. Kyoto University, Kyoto, Japan.

Oda, K., and N. Go. 1992. A model on the mechanism of tension development in an elastic muscle protein, connectin. *Biophys. Suppl. (Jpn.).* 32:S197*a*. (Abstr.)

Pfuhl, M., S. J. Winder, and A. Pastore. 1994. Nebulin, a helical actin binding protein. *EMBO J.* 13:1782–1789.

Pieronbon-Bormioli, S., R. Betto, and G. Salviati. 1989. The organization of titin (connectin) and nebulin in the sarcomeres: an immunocytolocalization study. *J. Muscle Res. Cell Motil.* 10:446–456.

Ridgway, E. B., A. M. Gordon, and D. A. Martyn. 1983. Hysteresis in the force-calcium relation in muscle. *Science.* 219:1075–1077.

Robinson, T. F., and S. Winegrad. 1977. Variation in thin filament length in heart muscle. *Nature.* 267:74–75.

Small, J. V., D. O. Fürst, and L.-E. Thornell. 1992. The cytoskeletal lattice of muscle cells. *Eur. J. Biochem.* 208:559–572.

Speakman, J. B. 1927. The intracellular structure of the wool fiber. *J. Textile Inst.* 18:T431–T453.

Takahashi, K., A. Hattori, R. Tatsumi, and K. Takai. 1992. Calcium-induced splitting of connectin filaments into α-connectin and a 1,200-kDa subfragment. *J. Biochem. (Tokyo).* 111:778–782.

Takemori, S. 1991. Relaxation of resting tension after stretch of skeletal muscle fibers. *Biophys. Suppl. (Jpn.).* 31:S247*a*. (Abstr.)

Tatsumi, R., and K. Takahashi. 1992. Calcium-induced fragmentation of skeletal muscle nebulin filaments. *J. Biochem. (Tokyo).* 112: 775–779.

Trinick, J. 1992. Understanding the functions of titin and nebulin. *FEBS Lett.* 307:44–48.

Wang, K. 1985. Sarcomere-associated cytoskeletal lattices in striated muscle: reviews and hypothesis. *In* Cell and Muscle Motility, Vol. 6. J. W. Shay, editor. Plenum Publishing Corp., New York. 315–369.

Wang, K., R. McCarter, J. Wright, J. Beverly, and R. Ramirez-Mitchell. 1991. Regulation of skeletal muscle stiffness and elasticity by titin isomers: a test of the segmental extension model of resting tension. *Proc. Natl. Acad. Sci. USA.* 88:7101–7105.

Wang, K., R. McCarter, J. Wright, J. Beverly, and R. Ramirez-Mitchell. 1993. Viscoelasticity of the sarcomere matrix of skeletal muscles. The titin-myosin composite filament is a dual-stage molecular spring. *Biophys. J.* 64:1161–1177.

Wang, K., and J. Wright. 1988. Architecture of the sarcomere matrix of skeletal muscle: immunoelectron microscopic evidence that suggests a set of parallel inextensible nebulin filaments anchored at the Z line. *J. Cell Biol.* 107:2199–2212.

Whiting, A., J. Wardale, and J. Trinick. 1989. Does titin regulate the length of muscle thick filaments? *J. Mol. Biol.* 205:263–268.

Wright, J., Q.-Q. Huang, and K. Wang. 1993. Nebulin is a full-length template of actin filaments in the skeletal muscle sarcomere: an immunoelectron microscopic study of its orientation and span with site-specific monoclonal antibodies. *J. Muscle Res. Cell Motil.* 14:476–483.

Yasuda, K., T. Anazawa, and S. Ishiwata. 1992. Elastic properties of myofibrils studied by a microscopic system newly developed for tension analysis. *J. Muscle Res. Cell Motil.* 13:478*a*. (Abstr.)

Yin, H. L., and T. P. Stossel. 1979. Control of cytoplasmic actin gel-sol transformation by gelsolin, a calcium-dependent regulatory protein. *Nature.* 281:583–586.